Heteronuclear decoupling with rotor-synchronized phase-alternated cycles

Andrea Simion, Tobias Schubeis, Tanguy Le Marchand, Mihai Vasilescu, Guido Pintacuda, Anne Lesage, Claudiu Filip

Heteronuclear decoupling with Rotor-Synchronized Phase-Alternated Cycles

Andrea Simion[1,2], Tobias Schubeis[2], Tanguy Le Marchand[2], Mihai Vasilescu[1], Guido Pintacuda[2], Anne Lesage[2] and Claudiu Filip[3,*]

[1]National Center for Magnetic Resonance, Faculty of Physics, Babeș-Bolyai University, 400084 Cluj-Napoca, Romania; [2]Centre de RMN à Très Hauts Champs de Lyon, Université de Lyon (UMR 5082 Centre National de la Research Scientifique/Ecole Normale Superiéure de Lyon/Université Claude Bernard Lyon 1), 69100 Villeurbanne, France; [3]National Institute for Research and Development of Isotopic and Molecular Technologies 400293 Cluj-Napoca, Romania *Corresponding author: claudiu.filip@itim-cj.ro

J. Chem. Phys. 157, 014202 (2022); https://doi-org /10.1063/5.0098135 - Copyright AIP

ABSTRACT

A new heteronuclear decoupling pulse sequence is introduced, dubbed ROtor-Synchronized Phase-Alternated Cycles (ROSPAC). It is based on a partial refocusing of the coherences (spin operator products or cross-terms) [Filip *et al.*, J. Mag. Reson. **176**, 2 (2005)] responsible for transverse spin-polarization dephasing, on the irradiation of a large pattern of radio-frequencies, and on a significant minimization of the cross-effects implying ^{1}H chemical-shift anisotropy. Decoupling efficiency is analyzed by numerical simulations and experiments and compared to that of established decoupling sequences [swept-frequency two-pulse phase-modulated (TPPM), TPPM, small phase incremental alternation (SPINAL), refocused Continuous-wave (CW^{Apa}), and Rotor-Synchronized Hahn-Echo pulse train (RS-HEPT)]. It was found that ROSPAC offers good ^{1}H offset robustness for a large range of chemical shifts and low radio-frequency (RF) powers, and performs very well in the ultra-fast magic-angle spinning (MAS) regime, where it is almost independent from RF power and permits it to avoid rotary-resonance recoupling conditions ($\nu_1 = n\nu_r$, $n = 1, 2$). It has the advantage that only the pulse lengths require optimization and has a low duty cycle in the pulsed decoupling regime. The efficiency of the decoupling sequence is demonstrated on a model microcrystalline sample of the model protein domain GB_1 at 100 kHz MAS at 18.8 T.

I. INTRODUCTION

Resolution and sensitivity are the traditional Achille's heel of solid-state nuclear magnetic resonance (ssNMR) spectroscopy. In static conditions, the chemical shift information is usually masked by the presence of strong anisotropic interactions, such as the chemical shift anisotropy (CSA), the homonuclear and heteronuclear dipolar couplings, or the quadrupolar couplings.[1,2] The effect of these anisotropic interactions can be averaged out in two ways: (i) by manipulating the spatial part of the Hamiltonian, spinning the sample around the magic angle, i.e., around an angle of 54.7° with respect to the external magnetic field,[3,4] or (ii) manipulating the spin part of the Hamiltonian, which is achieved by applying radio-frequency (RF) pulses. For heteronuclear dipolar interactions, which are the focus of this paper, a variety of heteronuclear decoupling pulse sequences have been developed over the last few decades.[7–10] Figure 1 presents the most used of them in a hierarchical form.

Continuous-wave (CW) heteronuclear decoupling has been the most commonly used heteronuclear sequence for many years.[13–13] CW variants, such as MLEV,[14] WALTS,[15] DIPSI,[16] and GARP,[17] and adiabatic inversion RF pulses, such as WURST[18] and SWIRL,[19] designed originally to decouple the isotropic heteronuclear J-couplings in solution nuclear magnetic resonance (NMR) experiments, were subsequently adapted to multiaspect signaling (MAS) NMR, at a high RF power to reduce the anisotropic interactions. The introduction of the two-pulse phase-modulated (TPPM) sequence in 1995 by Bennett *et al.*[8] was a key step, as it was shown to provide a significant improvement over CW decoupling in solids with dense homonuclear coupling networks. Since then, many variants of TPPM were designed that yielded improved decoupling performances, such as frequency-modulated and phase-modulated (FMPM),[20] small phase angle rapid cycling (SPARC),[21] small phase incremental alternation (SPINAL) and its variants,[22,23] amplitude-modulated TPPM

(AMPM),[24] GT-n sequences,[25] cosine-modulation (CM),[26] swept-frequency TPPM (sw-TPPM)[27] and its variants,[31–32] and refocused TPPM (rTPPM).[33]

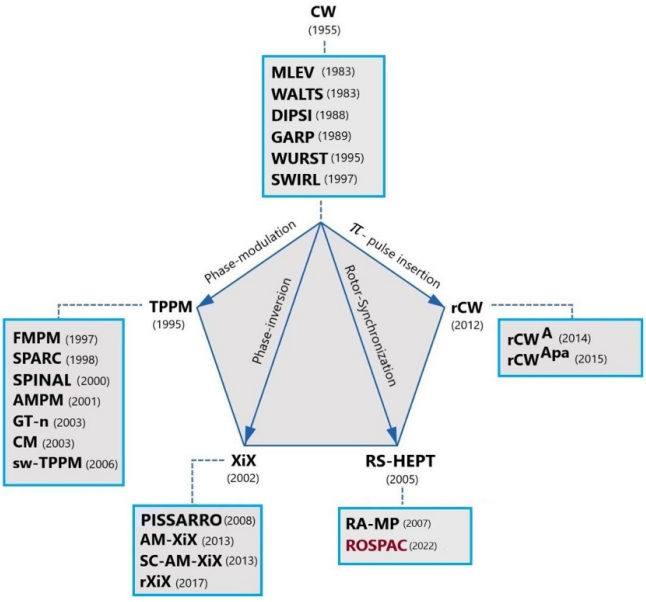

FIG. 1. Hierarchy of heteronuclear decoupling pulse sequences.

A second family was associated with the understanding of the importance of phase-inversion, which is incorporated in the X inverse X (XiX) sequence,[34,35] its variants, such as amplitude-modulated XiX (Am-XiX) and super-cycled amplitude-modulated XiX (SC-AM-XiX),[36] refocused XiX (rXiX),[37] and derivate sequences, such as a phase-inverted super-cycled sequence for attenuation of rotary resonance (PISSARRO).[38] A third family was based on the use of rotor-synchronized π-pulses, i.e., Rotor-Synchronized Hahn-Echo pulse train (RS-HEPT) sequence,[39,40] which, unlike the previous ones, uses time-reversal of the lowest-order effective Hamiltonian (i.e., $\text{Heff}^{(1)}$ from Eq. (9) in Ref. 41) under ultra-fast MAS, and not the additional modulation by the RF field, as the main decoupling mechanism. Derivate heteronuclear decoupling sequences were developed to remove the broadening of the spin-1/2 nuclei arising from the scalar coupling with quadrupolar nuclei, such as rotor-asynchronized multiple-pulse (RA-MP).[42]

A fourth family was conceived based on the demonstration that the insertion of rotor-synchronized π-pulses in the CW sequence can enhance the decoupling's efficiency. This leads to the development of the refocused CW (rCW) sequence,[43] and its variant, where π-pulses are non-rotor-synchronized, such as rCW^{A} or rCW^{Apa} sequences.[44,45] Recently, Equbal *et al.* demonstrated that the rCW^{Apa} sequence is robust regarding experimental parameters, such as pulse length and offset irradiation, and provides efficient heteronuclear decoupling in the low-power and fast MAS regimes.[46] Finally, a unified strategy of two-pulse-based heteronuclear decoupling sequences (UTPD)[47,48] was presented, demonstrating the importance of combined time- and phase-modulation. In the present work, we introduce a new heteronuclear decoupling pulse sequence, named Rotor-Synchronized Phase-Alternated Cycles (ROSPAC). Our results show that ROSPAC offers good ^{1}H offset robustness for a large chemical shift range under low-power irradiation, and performs well in the ultra-fast MAS regime, where it is almost independent of RF power, thus, avoiding rotary-resonance recoupling conditions. Moreover, being a pulsed sequence, ROSPAC has the advantage of a lower duty cycle compared to the conventional decoupling schemes relying on a continuous RF irradiation.

II. MATERIALS AND METHODS

A. Samples

98% uniform labeled ^{13}C,^{15}N-glycine, and ^{13}C,^{15}N-alanine were purchased from Cambridge Isotope Laboratories (CIL). The GB_1 (β_1 immunoglobulin binding domain of protein G) protein domain was expressed in *Escherichia coli* cultures, grown in an M9 medium containing 1,3-^{13}C-glycerol and

$^{15}NH_4Cl$ as sole carbon and nitrogen sources, purified by ion exchange and size-exclusion chromatography, and batch crystallized as described previously.[52–51]

B. Simulations

Simulations for ROSPAC and RS-HEPT sequences were performed using the SIMPSON simulation software package[52,53] for a CH_2 spin system assuming conditions of an 800 MHz NMR spectrometer, chemical shift anisotropy of protons of $\delta_{CSAH} = -2450$ Hz, and dipolar couplings of $\omega_{DC-H1}/2\pi = \omega_{DC-H2}/2\pi = -21.9$ kHz, $\omega_{DH1-H2}/2\pi = -23.3$ kHz. Isotropic chemical shifts, J-couplings, and asymmetry parameters were set to zero. The chemical shift anisotropy (CSA) of carbon spin was not taken into consideration, as it does not influence the decoupling performance. Simulations were carried out with 65 536 points and a spectral width of 12 000 Hz. Powder averaging was accomplished with a REPULSION scheme[54] employing 168 crystallite orientations and eight gamma angles.

C. Solid-state NMR spectroscopy

All spectra were recorded on a Bruker Avance III narrow-bore NMR spectrometer operating at a ^1H Larmor frequency of 800 MHz using a triple-resonance HCN 0.7 mm probe-head.
Measurements on glycine and alanine were carried out by applying a 90° pulse on the ^{13}C channel with a 3.5 μs duration, followed by the acquisition of the ^{13}C FID under heteronuclear decoupling (TPPM, sw-TPPM, SPINAL, rCW^{ApA}, or ROSPAC) applied on ^1H channel. For the case of rCW^{ApA}, optimizations were performed as described by Equbal *et al.*[46] The two-pulse phase difference was 15° for sw-TPPM and TPPM, while the phase alternation angles were $\alpha = 10°$ and $\beta = 5°$ for SPINAL and ROSPAC. The measurements were made at different rotation frequencies, i.e., 40, 60, and 100 kHz, respectively. All spectra were recorded with 16 scans, eight dummy scans, and a recycle delay of 10 s.
Spectra of the protein GB_1 were recorded at 100 and 60 kHz rotation frequencies, with a CP-HSQC pulse sequence[55] incorporating a non-selective spin-echo period on the ^{13}C channel (Fig. 10) with ROSPAC or sw-TPPM heteronuclear decoupling applied on the ^1H channel. The 90° pulse length was set to 1.25 μs on the ^1H channel and 5.18 μs on the ^{13}C channel. Contact times were 3 ms for the direct CP (i.e., ^1H -> ^{13}C) and 1 ms for the inverse CP (i.e., ^{13}C -> ^1H). Water suppression was performed with the MISSISSIPPI pulse scheme[56] applied on the ^1H channel without homospoil gradient, for a duration of 200 ms, and ^1H signal was recorded under Waltz-16 decoupling[15] applied on the ^{13}C channel at 10 kHz rf-field amplitude. NMR spectra were recorded with 16 scans in the former experiments, two dummy scans, and a recycle delay of 1 s.

III. RESULTS AND DISCUSSION

A. ROSPAC heteronuclear decoupling pulse sequence

Rotor-Synchronized Phase-Alternated Cycle (ROSPAC) (Fig. 2) is a heteronuclear decoupling pulse sequence designed for fast MAS NMR. It consists of 16 rotor-synchronized π-pulses, separated by a distance between them of $d = n\tau_r$, where τ_r is the rotor period and n is an integer number, having different values, depending on the rotation frequency, as discussed in the Result section. The 16 phases of the pulses are {10, 350, 15, 345, 20, 340, 15, 345, 350, 10, 345, 15, 340, 20, 345, 15} and were optimized experimentally. The sequence is based on partial refocusing of the coherences responsible for transverse spin-polarization dephasing, on increasing the resonance frequency range in the rotating frame, and on a significant minimization of the cross-terms between the ^1H chemical shift anisotropy and dipolar couplings. Its performance was analyzed both numerically and experimentally and compared to that of sw-TPPM, TPPM, SPINAL, rCW^{Apa}, and RS-HEPT.

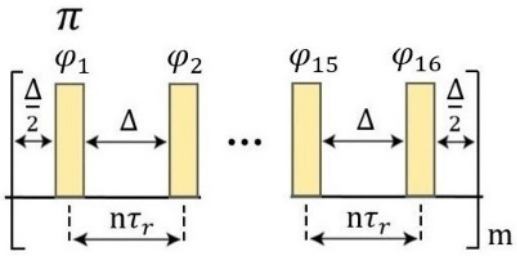

FIG. 2. ROSPAC heteronuclear decoupling pulse sequence.

B. Numerical simulations

1. Importance of phase alternation and supercycling

Robustness with respect to rotary-resonance conditions (i.e., $\nu_1 = n\nu_r$, where ν_r is the rotation frequency, ν_1 is the RF power, and n is a positive integer number) was observed when using two π-pulses separated by a rotor period (RS-HEPT decoupling sequence) [Fig. 3(a)]. The anti-periodic symmetry of single-spin operators (i.e., *Ix*, *Iy*, and *Iz*) in the interaction frame, in the sense defined in Ref. 57, leads to the minimization of cross-terms between ^{1}H–^{1}H homonuclear dipolar coupling and ^{1}H chemical-shift anisotropy (CSA) in the effective Hamiltonian. The introduction of such symmetry can be done by applying π-pulses separated by a rotor period, which, in the lowest order approximation of the effective Hamiltonian, refocuses the coherences responsible for dephasing transverse spin-polarization.[39] However, even if RS-HEPT has good performances in the ultra-fast MAS regime, good sensitivity and resolution can be achieved only in compounds with small ^{1}H chemical shielding parameters, and under high-power RF irradiation. By increasing the number of π-pulses to 16 and modulating their phases (as done in the ROSPAC decoupling sequence), a significant minimization of CSA is achieved, leading to a strong improvement in the decoupling efficiency, as can be seen in the simulated spectra of Fig. 3(b), where ROSPAC is compared with the RS-HEPT scheme previously introduced by us.[39]

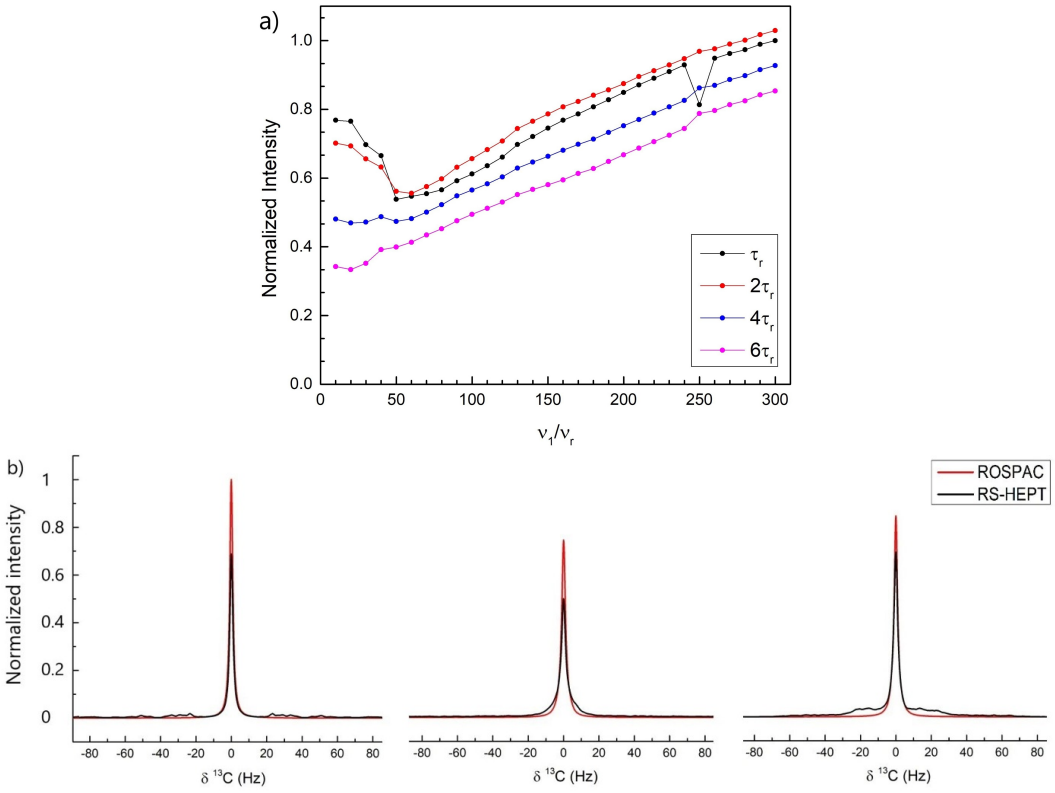

FIG. 3. (a) Normalized simulated peak height of a CH_2 group as a function of the radio frequency power, using RS-HEPT heteronuclear decoupling at 100 kHz rotation frequency for different distances between the π-pulses, i.e., τ_r, $2\tau_r$, $4\tau_r$, and $6\tau_r$ (peak intensity was normalized to that obtained with 300 kHz RF power and a distance between the π-pulses of τ_r). (b) Simulated carbon-13 spectra of a CH_2 group, using RS-HEPT (the distance between the π-pulses was τ_r) and ROSPAC (the distance between the π-pulses was $6\tau_r$) heteronuclear decoupling at 100 kHz rotation frequency and three different RF powers: 20, 70, and 160 kHz, respectively (peak intensity

was normalized to that obtained with 20 kHz RF power and 100 kHz rotation frequency using ROSPAC heteronuclear decoupling).

The proton line is partly inhomogeneous and, thus, difficult to saturate with a single frequency irradiation (e.g., using TPPM decoupling). Phase alternation overcomes this issue by enabling the irradiation of a larger pattern of frequencies in the rotating frame, i.e., over a broader range of different proton chemical shifts in the spectrum,[22] this effect being more significant in the low-power regime, where the RF power and chemical shifts are of the same order of magnitude. Moreover, if the π -pulses are separated by a rotor period, the irradiation pattern is extended in the ultra-fast MAS regime, proof being that better performances were obtained using ROSPAC with respect to SPINAL, which is also a phase-alternated sequence. The second key element that contributes to the enhanced efficiency is the supercycling. Interference effects that influence the decoupling performances will depend on (i) sample spinning frequency, (ii) modulation of irradiation frequencies, and (iii) static components of the RF Hamiltonian. In supercycled sequences, higher-order Fourier components play a significant role, being directly responsible for their superior performance in comparison to lower-order supercycle schemes.[58]

2. Choosing the number of π-pulses in the heteronuclear decoupling pulse sequence

The normalized peak height of the CH_2 group as a function of the number of π-pulses in the sequence was simulated for ROSPAC heteronuclear decoupling, at 60 kHz rotation frequency, with 10, 80, and 160 kHz RF powers (Fig. 4). For 2, 4, 8, 16, and 32 π-pulses, the phases were as follows: {10, 350}, {10, 350, 15, 345}, {10, 350, 15, 345, 20, 340, 15, 345}, {10, 350, 15, 345, 20, 340, 15, 345, 350, 10, 345, 15, 340, 20, 345, 15}, and {10, 350, 15, 345, 20, 340, 15, 345, 350, 10, 345, 15, 340, 20, 345, 15, 10, 350, 15, 345, 20, 340, 15, 345, 350, 10, 345, 15, 340, 20, 345, 15}, respectively. Using more than two π-pulses, and alternating the phases, an improvement was observed in the decoupling performance. The minimum number of π-pulses for which the same good performance was obtained in all the three RF power regimes, i.e., low-power, intermediate, and high-power regime, is 16. Increasing the number of pulses does not yield any improvement, i.e., a constant peak height of the CH_2 group was obtained. Therefore, 16 π-pulses were experimentally considered for the ROSPAC heteronuclear decoupling sequence.

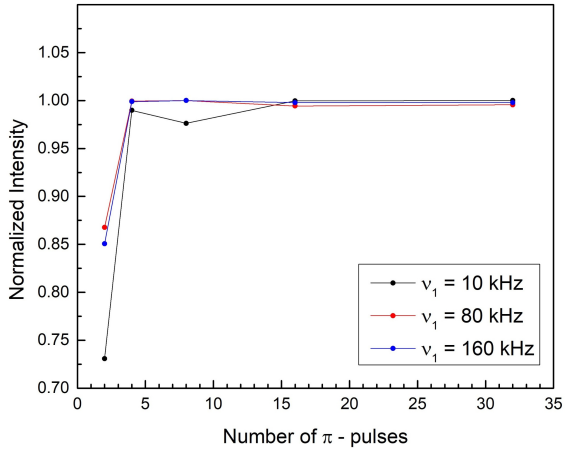

FIG. 4. Normalized simulated peak height of the CH_2 group as a function of the number of π-pulses in the sequence, using ROSPAC heteronuclear decoupling at 60 kHz MAS and 10, 80, and 160 kHz RF powers. Peak intensities were normalized to those obtained for each ν_1 power, i.e., 10, 80, or 160 kHz, respectively, at 60 kHz MAS.

C. Experimental results

1. Effect of delay between π-pulses

ROSPAC heteronuclear decoupling is a rotor-synchronized pulse sequence, i.e., the delay (Δ) between π-pulses satisfy the condition $\Delta = n\tau_r - p$, where n is an integer number, τ_r is the rotor period, and p is the π-pulses duration. The decoupling performance was evaluated experimentally for the CH_2 group of glycine, for different values of n, and at three rotation frequencies, i.e., 100,

60, and 40 kHz (Fig. 5). Note that the measurements started with RF powers for which a positive value of Δ was obtained, i.e., $p < n\tau_r$. Three decoupling regimes can be defined: (i) continuous-wave decoupling (i.e., Δ = 0), (ii) pulsed decoupling, where the distance between pulses is at least twice higher than the pulse length (i.e., Δ > 2p), and (iii) an intermediate regime, where the distance between π-pulses is close to the π-pulse length (i.e., Δ ≈ p). It was found that if we are in the intermediate regime, rotary-resonance conditions are avoided for ultra-fast MAS, and optimal decoupling efficiency is obtained independently from the rotation frequency. Good choices are n = 6 for 100 kHz rotation frequency, n = 4 for 60 kHz rotation frequency, and n = 2 for 40 kHz rotation frequency, these values being used for all the measurements from this article. As a general rule, n needs to be an integer number for which Δ ≈ p. In this regime, the effect of chemical shift anisotropy is extremely reduced or eliminated.

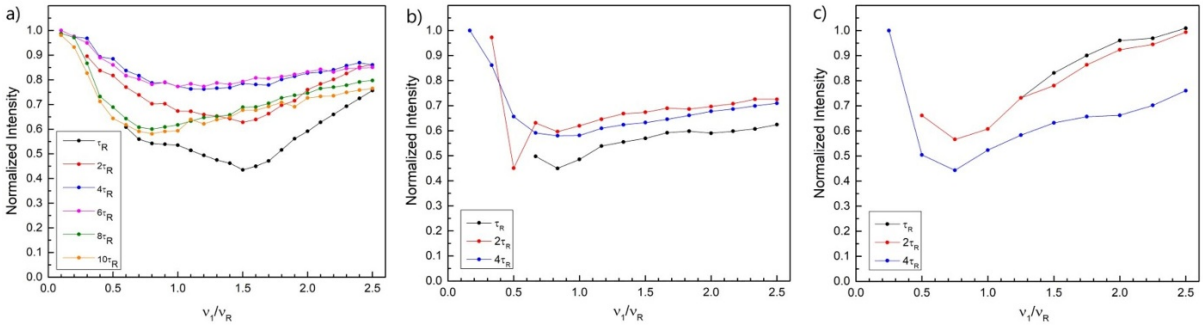

FIG. 5. Dependence of the normalized experimental peak height of the CH_2 group of glycine on the separation between π-pulses, as a function of the ratio between radio-frequency power and rotation frequency, using ROSPAC heteronuclear decoupling at 100 kHz (a), 60 kHz (b), and 40 kHz (c) MAS frequencies. Peak intensities were normalized to those obtained with ROSPAC decoupling at 10 kHz RF power at each particular MAS frequency, i.e., 100, 60, or 40 kHz, respectively.

2. Rotary-resonance conditions avoiding and closer to radio frequency power independence

In the ultra-fast (60 kHz and above) MAS regime, the number of resonance conditions increases, which limits the decoupling performance to a restricted range of RF powers. One solution to overcome this issue is to use a low power decoupling.[59,60] However, low-power heteronuclear decoupling schemes are quite intolerant to the offset of the carrier frequency. Developing heteronuclear decoupling sequences that avoid rotary-resonance conditions would be an alternative valuable option that possibly also enabling efficient decoupling at high RF powers.[61] Here, we note that two pulse sequences already exist that avoid the second-order rotary-resonance condition, namely, PISSARRO and rCW^{Apa}.[62,63] However, to the best of our knowledge, there are currently no heteronuclear decoupling schemes that prevent the interference observed at the first-order rotary-resonance condition, due to the reintroduction of the chemical shift anisotropy and dipolar coupling interactions. The performance of ROSPAC as a function of the RF power, with values ranging from 10 to 250 kHz was experimentally investigated at three spinning frequencies, i.e., 100, 60, and 40 kHz, and compared to that of existing heteronuclear decoupling schemes. More precisely, we compared ROSPAC with sw-TPPM by recording a series of carbon-13 spectra of L-alanine and measuring the intensity of the CH_3 and CH groups (Fig. 6). We also compared the performance of ROSPAC with that of TPPM, sw-TPPM, SPINAL, and rCW^{Apa} on the CH_2 group of glycine (Fig. 7).

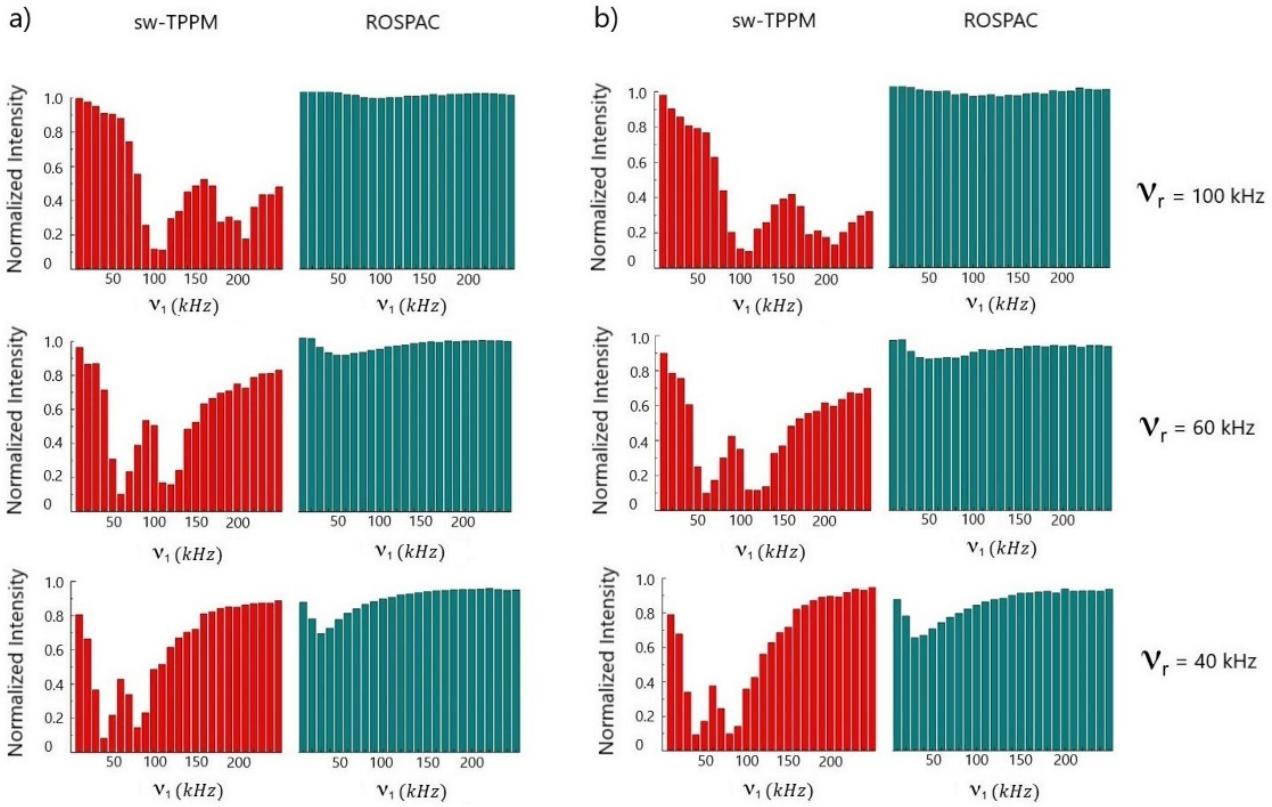

FIG. 6. Normalized experimental peak height of the CH_3 (a) and CH (b) groups of alanine as a function of the radio-frequency power, using sw-TPPM and ROSPAC heteronuclear decoupling at MAS frequencies ν_r of 100, 60, and 40 kHz. Peak intensities were normalized to those obtained with 10 kHz RF power of ROSPAC decoupling at 100 kHz MAS.

The data clearly show that for ROSPAC both first-order and second-order rotary-resonance conditions are avoided at each rotation frequency. Notably, a behavior almost RF power independent is observed for rotation frequencies $\nu_r \geq 60$ kHz. In addition, in this fast-spinning regime, the decoupling efficiency remains fairly constant over the whole RF range. Thus, if the MAS frequency is decreased, i.e., only 20% loss in signal intensity is observed for 40 kHz rotation frequency and 30 kHz RF power, compared to results obtained for 100 kHz rotation frequency, for measurements on CH_3 group of alanine. This is in contrast to sw-TPPM, where the loss in the signal intensity over the whole RF range was observed, up to 90% at the rotary-resonance recoupling conditions.

Figure 7 shows similar data recorded on glycine. Several additional decoupling sequences were compared. Again, relatively flat RF power profiles are observed at the three spinning frequencies. ROSPAC has similar performances as the rCW^{Apa} sequence in the low-power regime, while, in the intermediate and high RF power regimes, it outperforms all the analyzed pulse sequences, for ultra-fast MAS. At lower spinning frequencies, the signal intensity decreases, due to stronger homonuclear couplings between protons of the methylene group. Overall, at 100 kHz MAS, line widths as narrow as 0.39 ppm were obtained for the CH_2 group of glycine in the high-power regime (250 kHz RF) and 0.34 ppm in the low power regime (10 kHz RF). Our results prove that ROSPAC heteronuclear decoupling is a good choice for the fast and ultra-fast MAS regimes.

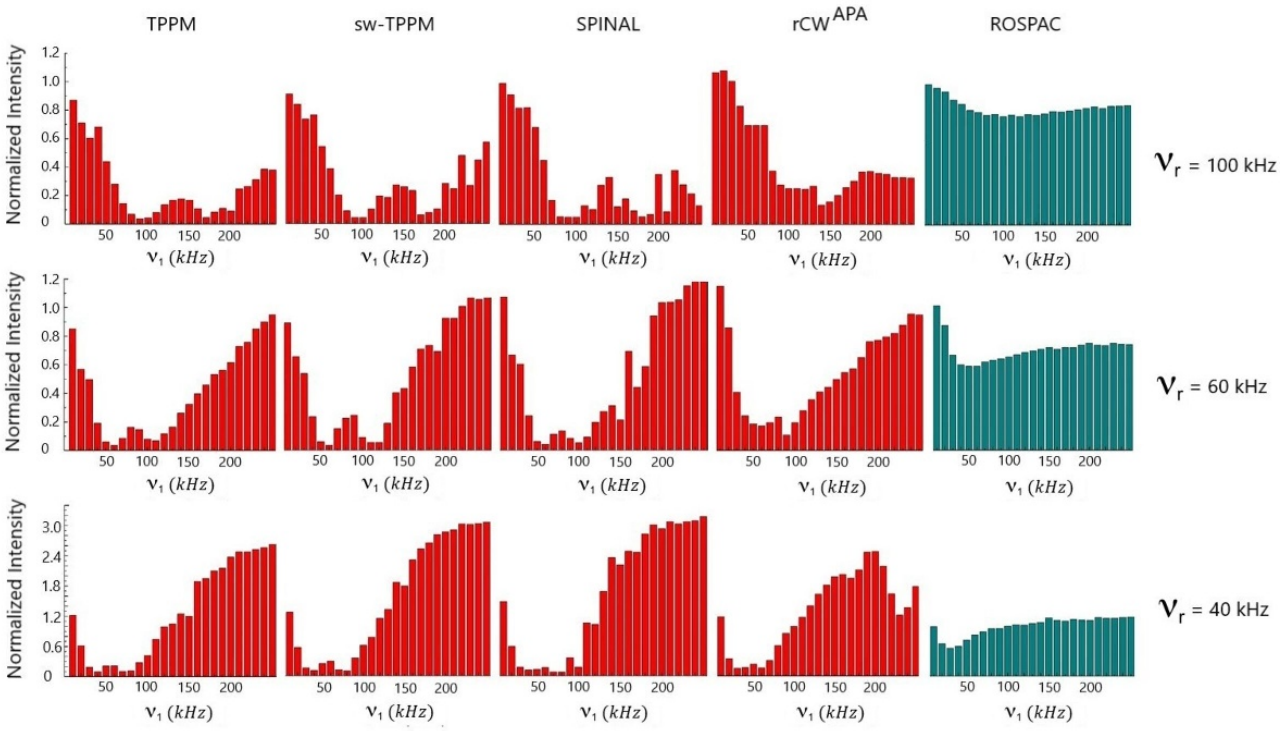

FIG. 7. Normalized experimental peak height of the CH_2 group of glycine as a function of the radio-frequency power, using TPPM, sw-TPPM, SPINAL, rCW^{ApA}, and ROSPAC heteronuclear decoupling at MAS frequencies ν_r of 100, 60, and 40 kHz. Peak intensities were normalized to those obtained with 20 kHz RF power of rCW^{Apa} decoupling at 100 kHz rotation frequency.

3. Robustness toward ^1H offset

In the low-power irradiation regime, decoupling performance is strongly dependent on the ^1H offset, a drop in the peak intensity up to 60% being found at small offsets around 4 ppm.[44] The offset dependence of the ROSPAC sequence was analyzed for three rotation frequencies, i.e., 100, 60, and 40 kHz, and three RF powers, i.e., 20, 70, and 160 kHz (Fig. 8). At 100 kHz rotation frequency, it was found that the low-power regime offers the best robustness regarding ^1H offset. Therefore, carrier frequency dependence was analyzed for 100 kHz rotation frequency and 20 kHz RF power for a larger offset scale, i.e., from −10 to 10 ppm, and compared to that obtained for various decoupling sequences discussed in this work (Fig. 9). It was found that ROSPAC performs slightly worse than SPINAL and rCW^{Apa} but better than TPPM or sw-TPPM decoupling, for small (<6 ppm) ^1H offsets. In the case of larger offsets, however, ROSPAC decoupling outperforms all the analyzed sequences, with a loss in intensity of about 30% at ±10 ppm. We expect this property to become relevant for future applications at ultra-high magnetic fields.

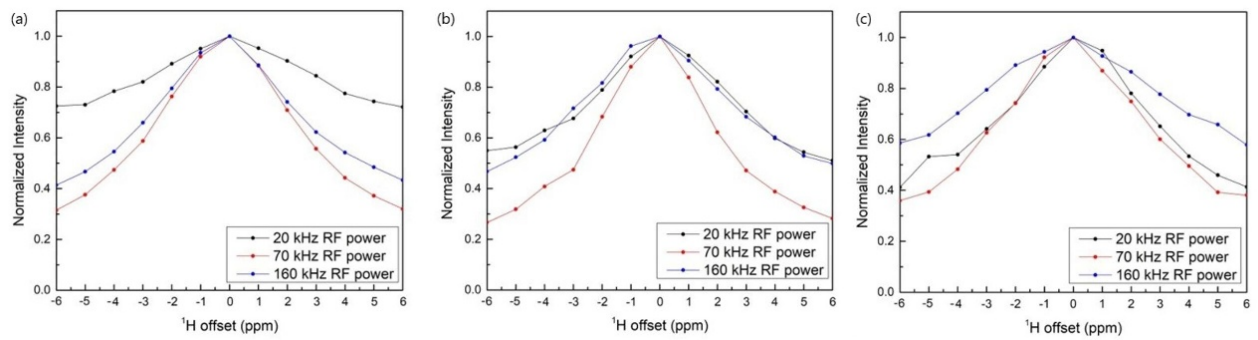

FIG. 8. Normalized experimental peak height of the CH_2 group of glycine as a function of the ^1H offset, using ROSPAC heteronuclear decoupling at 100 kHz (a), 60 kHz (b), and 40 kHz (c) rotation frequencies and 20, 70, and 160 kHz RF powers. Larmor frequency for ^1H nuclei was 800 MHz.

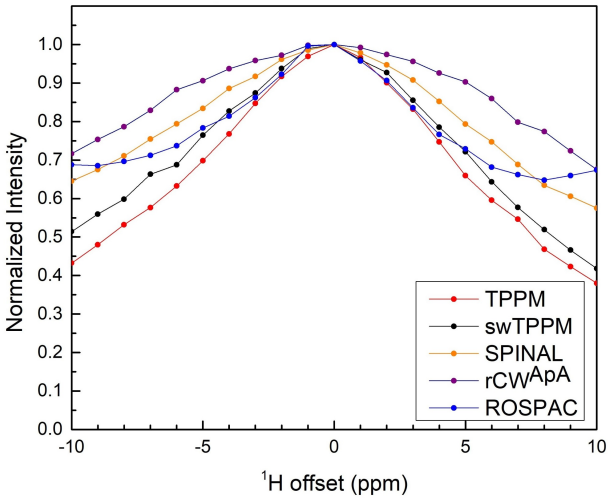

FIG. 9. Normalized experimental peak height of the CH_2 group of glycine as a function of the ^1H offset, using TPPM, sw-TPPM, SPINAL, rCW^{ApA}, and ROSPAC heteronuclear decoupling at 100 kHz rotation frequency and 20 kHz RF power. The Larmor frequency for ^1H nuclei was 800 MHz.

4. Applications to the β_1 domain of the immunoglobulin binding protein G (GB_1)

The decoupling efficiency of ROSPAC was then evaluated on a microcrystalline sample of the model protein domain GB_1 (β_1 immunoglobulin binding domain of protein G),[64] a prototypical example of a biosolid.

Figure 10 shows ^1H MAS NMR spectra recorded at 100 kHz MAS with a modified 2D CP-HSQC pulse sequence,[52] where a ^{13}C spin-echo of 100 ms was inserted instead of the t_1 period. This setup, coupled with the alternate 1,3-^{13}C-labeling scheme used here, is adapted to illustrate the efficiency of a decoupling sequence, since the experimental intensities depend uniquely on the heteronuclear T_2's for the particular decoupling sequence applied during the spin-echo. While at 10 kHz RF power, ROSPAC and sw-TPPM provide the same efficiency, it is evident that with 40 kHz RF power ROSPAC yields better performance, in agreement with the data obtained on glycine and alanine (see Figs. 6 and 7). Overall, these experiments demonstrate the efficiency toward a wide range of experimental conditions and straightforward applicability of ROSPAC decoupling for biomolecular MAS solid-state NMR spectroscopy.

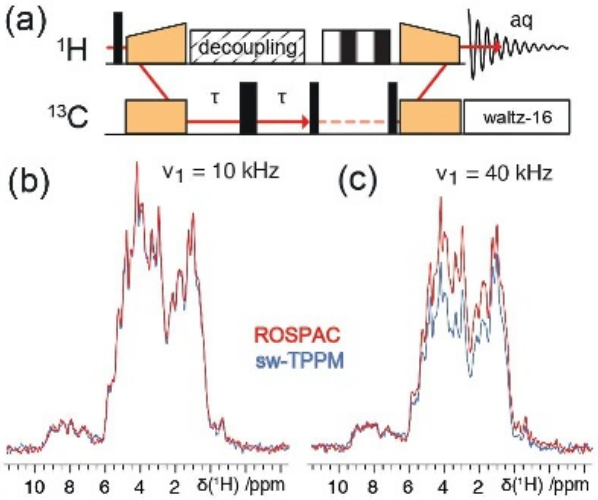

FIG. 10. (a) CP-HSQC scheme employed for the evaluation of heteronuclear decoupling in GB_1 and (b) and (c) experimental ^1H MAS NMR spectra of GB_1 protein recorded with sw-TPPM (blue lines) and ROSPAC (red lines) heteronuclear decoupling at 10 and 40 kHz RF powers and 100 kHz rotation frequency, on a 800 MHz spectrometer.

IV. CONCLUSIONS

In this work, a new heteronuclear decoupling pulse sequence was introduced. It was demonstrated that the alternation of phases in a supercycle rotor-synchronized π-pulses sequence leads to a

significant minimization of the chemical shift anisotropy and ^{1}H–^{1}H multi–spin interactions and irradiation of a larger pattern of RF frequencies. Moreover, in the intermediate decoupling regime, where the distance between π-pulses is close to the π-pulses length, both first and second-order rotary-resonance conditions are avoided. Our results show that ROSPAC heteronuclear decoupling offers improved performances, especially in the ultra-fast (60 kHz and above) MAS regime, in terms of RF power independence, ^{1}H offset robustness toward a large chemical shift range in the low-power regime, ease of optimization, and efficiency. Notably, there are two main applications where these advantages can be exploited: first, to study (bio)materials with large isotropic chemical shift dispersion in the proton spectrum, as paramagnetic materials;[65] and second, in dynamics experiments, e.g., for an accurate $T_{1\rho}$ relaxation mapping,[66] the sequence being used for decoupling during spin-lock. A more detailed analysis of the ROSPAC sequence using Floquet theory and the development of improved versions of this pulse sequence are currently being worked on and will be presented in a future paper.

SUPPLEMENTARY MATERIAL

See the supplementary material for SIMPSON scripts that are used to obtain the presented simulations.

ACKNOWLEDGMENTS

We acknowledge financial support from the European Union's Horizon 2020 Research and Innovation Program (Grant No. INFRAIA-02-2020 GA 101008500 "PANACEA" to G.P. and A.L. and Grant No. INFRAIA-01-2018-2019 GA 871037 "iNext Discovery" to G.P.), the European Research Council (Grant No. ERC-CoG-2015 GA 648974 "P-MEM-NMR" to G.P.), and the CNRS (Grant No. FR 2054). A.S. acknowledges a research fellowship from the World Federation of Scientists (WFS), CERN, Geneva, Switzerland, and a Scholarship from the Faculty of Physics, Babeș-Bolyai University, Cluj-Napoca, Romania. We thank Professor M. Ernst for helpful suggestions and discussions.

AUTHOR DECLARATIONS

Conflict of Interest

The authors have no conflicts to disclose.

DATA AVAILABILITY

The data that support the findings of this study are available from the corresponding author upon reasonable request.

REFERENCES

[1] M.H. Levitt, G. Bodenhausen, and R.R. Ernst, J. Magn. Reson. **53**, 443 (1983).
[2] J.S. Waugh, J. Magn. Reson. **50**, 30 (1982).
[3] M. H. Levitt, John Wiley & Sons, New York, (2008).
[4] R. R. Ernst, G. Bodenhausen, Claredon Press, Oxford, (1987).
[5] E. Andrew, A. Bradbury and R. Eades, Nature, **183**, (1959).
[6] I. J. Lowe, Phys. Rev. Lett., **2**, 7, (1959).
[7] M. Ernst, J. Magn. Reson. **162**, 1, (2003).
[8] A.E. Bennett, C.M. Rienstra, M. Auger, K. V. Lakshmi, and R.G. Griffin, J. Chem. Phys. **103**, 6951, (1995).
[9] A. Khitrin and B.M. Fung, J. Chem. Phys. **112**, 2392 (2000).
[10] P. Hodgkinson, Prog. Nucl. Magn. Reson. Spectrosc. **46**, 197 (2005).
[11] S. Paul, N.D. Kurur, and P.K. Madhu, J. Magn. Reson. **207**, 140 (2010).
[12] P.K. Madhu, Isr. J. Chem. **54**, 25 (2014).
[13] H.J. Reich, M. Jautelat, M.T. Messe, F.J. Weigert, and J.D. Roberts, J. Am. Chem. Soc. **91**, 7445 (1969).

[14] B. Birdsall, N. J. M. Birdsall and J. Feeney, J. Chem. Soc., Chem. Commun., 6 (1972).
[15] R. Ernst, J. Chem. Phys. **45**, 3845 (1966).R
[16] J. W. M. Jacobs, J. W. M. Van Os and W. S. Veeman, J. Magn. Reson., **51**, 1 (1983).
[17] A.J. Shaka, J. Keeler, T. Frenkiel, and R. Freeman, J. Magn. Reson. **52**, 335 (1983).
[18] A.J. Shaka, C.J. Lee, and A. Pines, J. Magn. Reson. **77**, 274 (1988).
[19] R. W. Dykstra, J. Magn. Reson. **82**, 347 (1989).
[20] Ē. Kupče and R. Freeman, J. Magn. Reson. Ser. A **115**, 273 (1995).
[21] Ē. Kupče and R. Freeman, J. Magn. Reson. Ser. A **125**, 376 (1997).
[22] A.E. Bennett, C.M. Rienstra, M. Auger, K.V. Lakhsmi and R.G. Griffin, J. Chem. Phys, **103**, 6951 (1995).
[23] Z. Gan and R.R. Ernst, Solid State Nucl. Magn. Reson. **8**, 153 (1997).
[24] Y. L. Yu and B. M. Fung, J. Magn. Reson. **130**, 317 (1998).
[25] B.M. Fung, A.K. Khitrin, and K. Ermolaev, J. Magn. Reson. **142**, 97 (2000).
[26] C.V. Chandran and T. Bräuniger, J. Magn. Reson. **200**, 226 (2009).
[27] K. Takegoshi, J. Mizokami, and T. Terao, Chem. Phys. Lett. **341**, 540 (2001).
[28] G. Gerbaud, F. Ziarelli, and S. Caldarelli, Chem. Phys. Lett. **377**, 1 (2003).
[29] G. De Paëpe, B. Eléna, and L. Emsley, J. Chem. Phys. **121**, 3165 (2004).
[30] R.S. Thakur, N.D. Kurur, and P.K. Madhu, Chem. Phys. Lett. **426**, 459 (2006).
[31] R.S. Thakur, N.D. Kurur, and P.K. Madhu, J. Magn. Reson. **185**, 264 (2007).
[32] C. Vinod Chandran, P.K. Madhu, N.D. Kurur, and T. Bräuniger, Magn. Reson. Chem. **46**, 943 (2008).
[33] C. Vinod Chandran, P.K. Madhu, P. Wormald, and T. Bräuniger, J. Magn. Reson. **206**, 255 (2010).
[34] C. Augustine and N. D. Kurur, Magn. Reson. Chem., **48**, 798 (2010).
[35] C. Augustine and N.D. Kurur, J. Magn. Reson. **209**, 156 (2011).
[36] A. Equbal, S. Paul, V.S. Mithu, J.M. Vinther, N.C. Nielsen, and P.K. Madhu, J. Magn. Reson. **244**, 68 (2014).
[37] A. Detken, E.H. Hardy, M. Ernst, and B.H. Meier, Chem. Phys. Lett. **356**, 298 (2002).
[38] M. Ernst, A. Samoson, and B.H. Meier, J. Magn. Reson. **163**, 332 (2003).
[39] V. Agarwal, T. Tuherm, A. Reinhold, J. Past, A. Samoson, M. Ernst and B. H. Meier, Chem. Phys. Lett., **583**, 1 (2013).
[40] M.G. Jain, K.N. Sreedevi, A. Equbal, P.K. Madhu, and V. Agarwal, J. Magn. Reson. **284**, 59 (2017).
[41] M. Weingarth, P. Tekely, and G. Bodenhausen, Chem. Phys. Lett. **466**, 247 (2008).
[42] X. Filip, C. Tripon and C. Filip, J. Magn. Reson **176**, 2 (2005).
[43] J. M. Griffin, C. Tripon, A. Samoson, C. Filip and S. P. Brown, Magn. Reson. Chem. **45**, S1, (2007).
[44] K.O. Tan, V. Agarwal, B.H. Meier, and M. Ernst, J. Chem. Phys. **145**, (2016).
[45] L. Delevoye, J. Trébosc, Z. Gan, L. Montagne, and J.P. Amoureux, J. Magn. Reson. **186**, 94 (2007).
[46] J. M. Vinther, A. B. Nielsen, M. Bjerring, E. R. H. Van Eck, A. P. M. Kentgens, N. Khaneja and N. C. Nielsen, J. Chem. Phys. **137**, 214202 (2012);
[47] A. Equbal, S. Paul, V.S. Mithu, P.K. Madhu, and N.C. Nielsen, J. Magn. Reson. **246**, 104 (2014).
[48] A. Equbal, M. Bjerring, P.K. Madhu, and N.C. Nielsen, Chem. Phys. Lett. **635**, 339 (2015).
[49] A. Equbal, P.K. Madhu, B.H. Meier, N.C. Nielsen, M. Ernst, and V. Agarwal, J. Chem. Phys. **146**, (2017). [50] A. Equbal, M. Bjerring, P.K. Madhu, and N.C. Nielsen, J. Chem. Phys. **142**, (2015).
[51] A. Equbal, M. Bjerring, P. K. Madhu and N. C. Nielsen, J. Chem. Phys. **150**, (2019).
[52] M. Cai, Y. Huang, R. Craigie, and G.M. Clore, J. Biomol. NMR **73**, 743 (2019).
[53] G. L. Rosano and E. A. Ceccarelli, Front. Microbiol. **5**, 1 (2014).
[54] W.T. Franks, D.H. Zhou, B.J. Wylie, B.G. Money, D.T. Graesser, H.L. Frericks, G. Sahota, and C.M. Rienstra, J. Am. Chem. Soc. **127**, 12291 (2005).
[55] M. Bak, J.T. Rasmussen, and N.C. Nielsen, J. Magn. Reson. **147**, 296 (2000).
[56] Z. Tošner, R. Andersen, B. Stevensson, M. Edén, N.C. Nielsen, and T. Vosegaard, J. Magn. Reson. **246**, 79 (2014).
[57] M. Bak and N.C. Nielsen, J. Magn. Reson. **125**, 132 (1997).
[58] E.K. Paulson, C.R. Morcombe, V. Gaponenko, B. Dancheck, R.A. Byrd, and K.W. Zilm, J. Am. Chem. Soc. **125**, 15831 (2003).
[59] D. H. Zhou and C. M. Rienstra, J. Magn. Reson., **192**, 1, (2008).
[60] A. Equbal, R. Shankar, M. Leskes, S. Vega, N.C. Nielsen, and P.K. Madhu, J. Chem. Phys. **146**, (2017).
[61] R. Garg, M.K. Pandey, and R. Ramachandran, J. Chem. Phys. **155**, 10, (2021).
[62] I. Frantsuzov, S.K. Vasa, M. Ernst, S.P. Brown, V. Zorin, A.P.M. Kentgens, and P. Hodgkinson, ChemPhysChem **18**, 394 (2017).

[63] M. Ernst, A. Samoson, B. H. Meier, **348**, 3-4, (2001).
[64] A. Equbal, M. Bjerring, K. Sharma, P. K. Madhu and N. C. Nielsen, Chem. Phys. Lett. **644**, 243, (2016).
[65] K. Sharma, P.K. Madhu, and V. Agarwal, J. Magn. Reson. **270**, 136 (2016).
[66] R.N. Purusottam, G. Bodenhausen, and P. Tekely, Chem. Phys. Lett. **614**, 220 (2014).
[67] K.O. Tan, V. Agarwal, B.H. Meier, and M. Ernst, J. Chem. Phys. **145**, (2016).
[68] H.N.B. Moseley, L.J. Sperling, and C.M. Rienstra, J. Biomol. NMR **48**, 123 (2010).
[69] M.J. Willans, D.N. Sears, and R.E. Wasylishen, J. Magn. Reson. **191**, 31 (2008).
[70] D.M. Korzhnev, M. Billeter, A.S. Arseniev, and V.Y. Orekhov, Prog. Nucl. Magn. Reson. Spectrosc. **38**, 197 (2001).